Final Report

Surface-Induced Dissociation versus Collision-Induced Dissociation: The Bruker 7 Tesla Fourier transform ion-cyclotron resonance (FTICR) mass spectrometer was modified to insert a surface inside the cell for ion-surface collisions leading to the dissociation of impacting ions. The surface was mounted in the ICR cell through an aperture in the back trapping plate. Necessary modifications were made to the software/ hardware to collide the ions brought into the cell and trap the resulting fragment and undissociated primary ions inside the cell. The trapping plates were also ramped to determine kinetic energy distributions of these ions. We used self assembled monolayer (SAM) surface of FC_{12} alkanethiol ($CF_3(CF_2)_9(CH_2)_2SH$) on gold surface formed by immersing it in a 1 mM ethanol solution of the surface material. We first studied surface-induced dissociation (SID) of benzene and chromium hexacarbonyl ions as test cases for the instrument since the energetics and dissociation dynamics of these ions is very well understood from photoelectron photoion coincidence (PEPICO), photoionization (PI) and several other studies. Furthermore, their SID processes have been previously investigated by us on our 3 Tesla FT ICR and by others using different instrumentations. After these studies established the suitability and ease of performing SID experiments on this instrument, we began a systematic study of the SID of small protonated peptides formed by electrospray ionization. A series of small alanine (A) containing peptides, viz., AA, AAA, AAAA, AAAAA and PAAAA were used in the present study.

In the absence of any direct comparisons of the SID processes with the commonly used technique of tandem mass spectrometry of collision-induced dissociations (CID) via collisions with a neutral gas, we made a comparative study of CID and SID using the same protonated peptides. Since multiple collisions are often used to enhance dissociation efficiency in CID, we performed CID under single as well as multiple collisional activation (MCA) conditions. Both on-resonance and sustained off-resonance irradiation (SORI) excitation were used for CID experiments. Kinetic energy of the ions was varied by changing peak-to-peak voltage applied to the excitation plates.

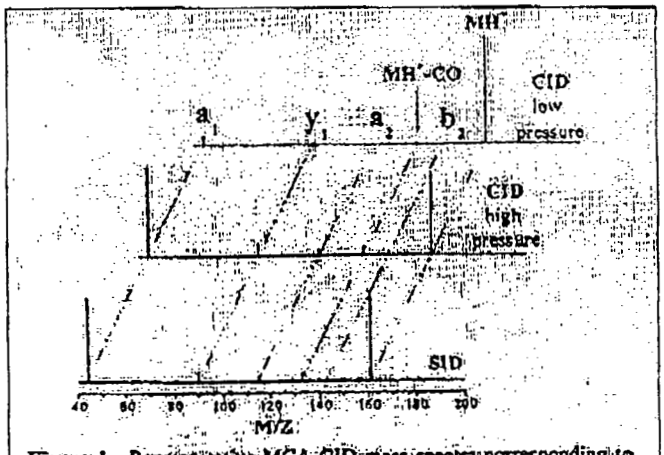

Figure 1. Representative MCA-CID mass spectra corresponding to the CM energy of 3 eV (top panel) and SID spectrum at 11.5 eV incident collision energy (bottom panel).

DOE Patent Clearance Granted

MP Dvorscak 5-16-01

Mark P. Dvorscak
(630) 252-2393
E-mail: mark.dvorscak@ch.doe.gov
Office of Intellectual Property Law
DOE Chicago Operations Office

DISCLAIMER

Figure 1 shows the energy resolved MCA-CID spectra of AAH^+ at two different pressures corresponding to 5 and 15 collisions and its SID spectrum at 11.5 eV impact energy. It is interesting that high pressure CID at 3 eV CM energy is very similar to the SID spectrum at 11.5 eV ion collision energy in the laboratory frame of reference. Since it is not easy to determine the CM collision energy in SID, this figure suggested to use an "effective" CM energy for SID using an arbitrary neutral of mass M_N to compare the SID and CID curves using the same relationship as for CID. By adjusting MN until the best overlap between the rising part of the SID and CID curves of a major primary fragment was obtained. By doing so, the best overlap between the SID and MCA-CID fragmentation efficiency curves for most cases is obtained for $M_N = 46$ for AAH^+. When extended to other peptides mentioned above, we estimate an average value of 43 ± 3 for the neutral collision partner to give similar fragmentations in the two processes. Figures 2 and 3 show a comparison of the fragmentation efficiency curves for $AAAAAH^+$ and $PAAAAH^+$, respectively, which are very similar under both excitation conditions.

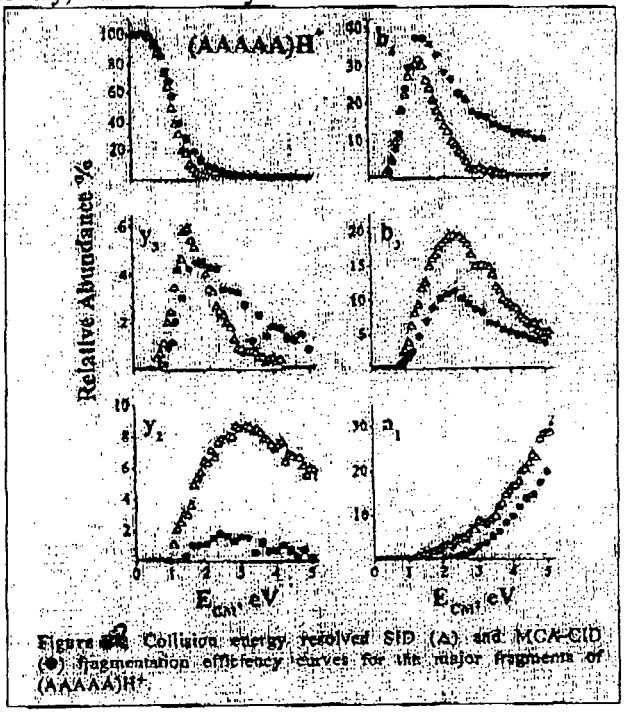

Figure 2. Collision energy resolved SID (▲) and MCA-CID (●) fragmentation efficiency curves for the major fragments of $(AAAAA)H^+$.

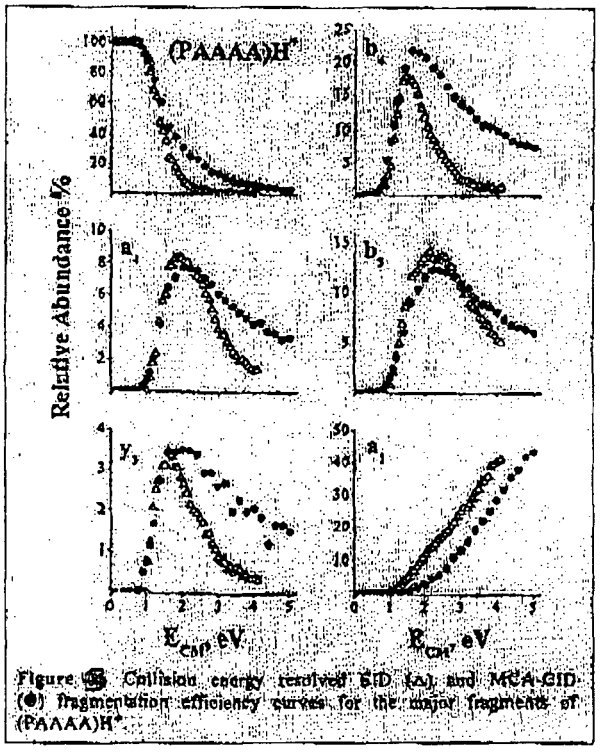

Figure 3. Collision energy resolved SID (▲) and MCA-CID (●) fragmentation efficiency curves for the major fragments of (PAAAA)H+.

The results described above show that multiple collision activation and SID both result in very similar energy resolved fragmentation efficiency curves except at higher collision energies where SID seems to be more effective than CID. These differences are easily rationalized based upon internal energy distributions in the two activation processes as discussed later. The main difference between the SID and MCA-CID is the relative abundances of y_2 ions produced from tri- and penta- alanine which is much higher in SID. This difference is explained by competing dissociation channels available in MCA-CID process since energy is transferred in smaller increments in this case. Collision energy resolved total fragmentation efficiency curves (Fig. 4) as a function of the "effective" CM collision energy show an interesting feature that dialanine requires much higher energy for fragmentation than other peptides used in the present study.

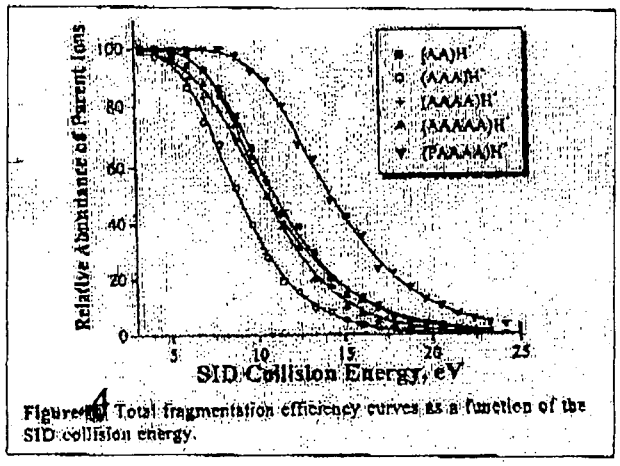

Figure 4. Total fragmentation efficiency curves as a function of the SID collision energy.

Theoretical Modeling: Since mass spectrum of a molecule can be calculated if its fragmentation sequence, energy dependent rate constants of each fragmentation process and the internal energy distribution of the fragmenting ions are known along with the measurement time scale for the mass spectrometer. The internal energy distribution of an activated ion can thus be estimated if rests of the parameters are known. Energy dependent microcanonical dissociation rate constants for all fragmentations are calculated by the RRKM/ QET theories of unimolecular dissociations. Fragmentation probability as a function of the internal energy of the parent ion and the experimental observation time (t_r), $F(E, t_r)$ is calculated based upon the reaction scheme and their energetics. The energy deposition function is described by the following analytical expression:

$$P(E, E_{coll}) = (E - \Delta)^l \exp[-(E - \Delta)/f(E_{coll})]/C$$

Where l and Delta are variable parameters, $C = \sum (l + 1)[f(E_{coll})]^{l+1}$ is a normalization factor and f(Ecoll) has the following form:

$$F(E_{coll}) = A_2 E_{CM}^2 + A_1 E_{CM} + A_0$$

Where A_0, A_1 and A_2 are variable parameters. For MCA-CID results A_0 was replaced with $E_{th}/(l + 1)$ where E_{th} is the average thermal energy of the protonated peptide at 298 K. E_{coll} equals the collision energy for SID experiments and the maximum CM collision energy for MCA-CID experiments.

Since collisional activation in both CID and SID produce ions with a wide range of internal energy distribution, $P(E, E_{CM})$, the contribution of ions having internal energy E to the observed signal intensity for a particular reaction channel, i, equals $F_i(E, t_r)P(E, E_{CM})$. Integrating over all internal energies yields an overall signal intensity at a given CM energy as follows:

$$I_i(E_{CM}) = \int_0^\infty F_i(E,t_r)\, P(E, E_{CM})\, dE$$

The variable parameters were adjusted until the best fit to experimental fragmentation efficiency curves was obtained. In the absence of critical energies for various dissociations and their activation entropies, we varied these also to give the best fit. We used the same approach to model the fragmentation efficiency curves for both SID and MCA-CID experiments except the reaction times taken as1 second and 5 seconds, respectively, for the two processes.

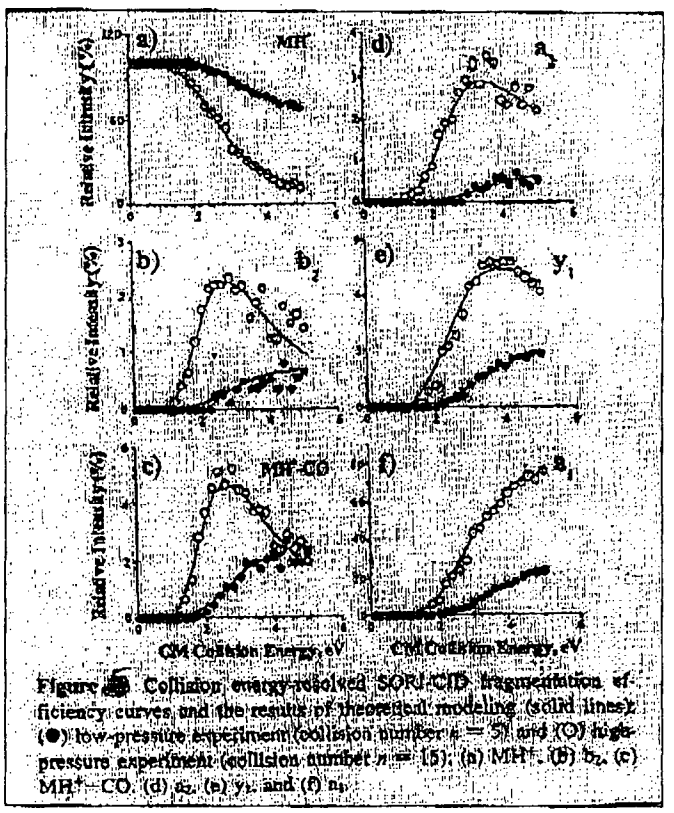

Figure 4. Collision energy-resolved SORI-CID fragmentation efficiency curves and the results of theoretical modeling (solid lines): (●) low-pressure experiment (collision number $n = 5$) and (○) high-pressure experiment (collision number $n = 15$); (a) MH^+, (b) b_2, (c) $MH^+ - CO$, (d) a_2, (e) y_1, and (f) a_1.

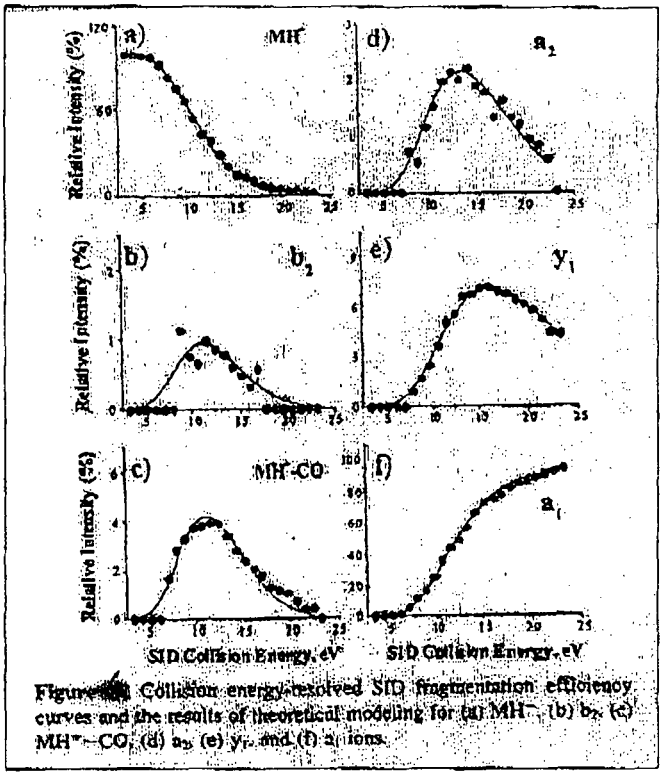

Figure 5. Collision energy-resolved SID fragmentation efficiency curves and the results of theoretical modeling for (a) MH^+, (b) b_2, (c) MH^+-CO, (d) a_2, (e) y_1, and (f) a_1 ions.

Figures 5 and 6 present the collision energy resolved SORI-CID and SID fragmentation efficiency curves and the results of theoretical modeling (solid lines), respectively, for AAH^+. The agreement between the experiments and the model is fairly good. The fact that both CID and SID experiments could be reproduced using the same model suggests that these two activation techniques are very similar in nature. This is further supported by the internal energy distributions, shown in Fig. 7, that gave the best fit to the SID and high pressure multiple collision (collision number 15) experiments. The only difference being slight asymmetry and shift towards higher energy in SID distributions (dashed lines). Using this model we can now calculate the most probable internal energy deposited in these ions. For protonated Dialanine, Fig. 8 shows that most probable energy deposited increases linearly with the E_{CM} while it begins to reach a plateau in the case of CID and this may be the reason for the small differences in the two cases at higher energies as mentioned in the earlier section.

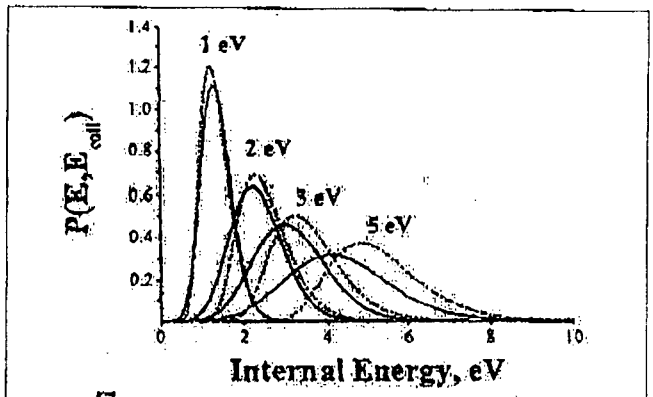

Figure 7. Internal energy distributions upon multiple-collision (solid lines) and ion–surface impact (dashed lines). MCA-CID distributions corresponding to the maximum center-of-mass (CM) energy of 1, 2, 3, and 5 eV. The SID collision energy was converted to an "effective" CM energy assuming the mass of neutral encounter on the surface of 46 amu.

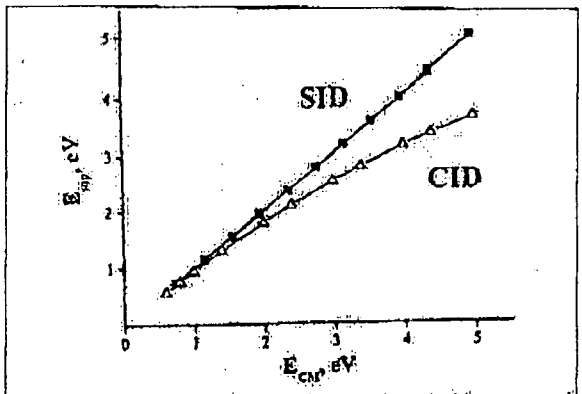

Figure 8. The most probable internal energy deposited in protonated dialanine by multiple collisions (Δ) and ion–surface interaction (■). E_{dep} is plotted as a function of the maximum center-of-mass (CM) collision energy for MCA-CID and the "effective" CM energy for SID (see text for discussion).

A direct comparison of the two activation techniques on the same instrument provided invaluable insights into the similarities and differences between these two. Our results suggest that internal energy distributions of ions activated by ion-surface collision and multiple collision ion- gaseous neutral collisions are quite comparable. Our results also suggest that in ion-surface collisions, the ion collides only with a small fraction of the SAM chain making it effectively a process very similar to CID.